Chemico-Biological Interactions 239 (2015) 153–163

Contents lists available at ScienceDirect

Chemico-Biological Interactions

journal homepage: www.elsevier.com/locate/chembioint

A systems toxicology approach on the mechanism of uptake and toxicity of MWCNT in *Caenorhabditis elegans*

Hyun-Jeong Eom [a], Carlos P. Roca [b], Ji-Yeon Roh [a], Nivedita Chatterjee [a], Jae-Seong Jeong [a], Ilseob Shim [c], Hyun-Mi Kim [c], Phil-Je Kim [c], Kyunghee Choi [c], Francesc Giralt [b], Jinhee Choi [a,*]

[a] School of Environmental Engineering, Graduate School of Energy and Environmental System Engineering, University of Seoul, Seoul 130-743, Republic of Korea
[b] Departament d'Enginyeria Quimica, Universitat Rovira i Virgili, Tarragona, Catalunya, Spain
[c] Risk Assessment Division, National Institute of Environmental Research, Incheon 404-708, Republic of Korea

ARTICLE INFO

Article history:
Received 18 November 2014
Received in revised form 5 May 2015
Accepted 21 June 2015
Available online 22 June 2015

Keywords:
Multiwall carbon nanotubes
Caenorhabditis elegans
Phagocytosis
Adverse outcome pathway
Systems toxicology

ABSTRACT

The increased volumes of carbon nanotubes (CNTs) being utilized in industrial and biomedical processes carries with it an increased risk of unintentional release into the environment, requiring a thorough hazard and risk assessment. In this study, the toxicity of pristine and hydroxylated (OH–) multiwall CNTs (MWCNTs) was investigated in the nematode *Caenorhabditis elegans* using an integrated systems toxicology approach. To gain an insight into the toxic mechanism of MWCNTs, microarray and proteomics were conducted for *C. elegans* followed by pathway analyses. The results of pathway analyses suggested endocytosis, phagocytosis, oxidative stress and endoplasmic reticulum (ER) stress, as potential mechanisms of uptake and toxicity, which were subsequently investigated using loss-of-function mutants of genes of those pathways. The expression of phagocytosis related genes (i.e. *ced-10* and *rab-7*) were significantly increased upon exposure to OH-MWCNT, concomitantly with the rescued toxicity by loss-of-function mutants of those genes, such as *ced-10(n3246)* and *rab-7(ok511)*. An increased sensitivity of the *hsp-4(gk514)* mutant by OH-MWCNT, along with a decreased expression of *hsp-4* at both gene and protein level suggests that MWCNTs may affect ER stress response in *C. elegans*. Collectively, the results implied phagocytosis to be a potential mechanism of uptake of MWCNTs, and ER and oxidative stress as potential mechanisms of toxicity. The integrated systems toxicology approach applied in this study provided a comprehensive insight into the toxic mechanism of MWCNTs in *C. elegans*, which may eventually be used to develop an "Adverse Outcome Pathway (AOP)", a recently introduced concept as a conceptual framework to link molecular level responses to higher level effects.

1. Introduction

The extensive use of engineered nanomaterials (eNM) in industrial and biomedical processes may lead to their unintentional release into the environment, requiring a thorough hazard and risk assessment. For example, carbon nanotubes (CNTs) have found application in sensors and electronic devices, as well as in catalysis, wastewater treatment and drug delivery, due to their attractive structural, mechanical, electrical and optical properties [1,2]. Thus, the potential hazards of CNT in human and environmental health have been investigated in numerous studies [3–5]. Most toxicity studies of CNTs have focused on *in vivo* toxicity through respiratory exposure pathways or *in vitro* assays relating to pulmonary cells, due to the similarity of the structure of CNTs to that of asbestos [6–8]. As potential mechanisms of toxicity of CNT, most studies emphasize oxidative stress, inflammation, and fibrosis, etc. [6,9]. Recently developed systemic and integrated omics approaches can provide a comprehensive insight into the mechanism of toxicity, which is particularly valuable when investigating the toxicity of new chemicals, whose mode of action is not fully understood, such as with eNMs. So far, only limited studies are available on the ecotoxicity of CNT [10–12], and fewer again on the mechanisms of toxicity for non-mammalian model species [13,14].

Here, the comprehensive molecular mechanism of toxicity of multiwall carbon nanotubes (MWCNTs) was thoroughly investigated in the nematode *Caenorhabditis elegans*, using transcriptomics and proteomics. *C. elegans* has become a popular model in (eco)toxicology and research [15] and is also being widely used in nano(eco)toxicology as was recently reviewed by Choi et al. [16]. *C. elegans* offers several advantages and in the context of

* Corresponding author.
E-mail address: jinhchoi@uos.ac.kr (J. Choi).

http://dx.doi.org/10.1016/j.cbi.2015.06.031
0009-2797/

nanotoxicology. One of the advantages of *C. elegans* lies in the possibility of studying organismal uptake of eNMs and their distribution in whole organisms, due to its small size and transparency. *C. elegans* also offers the ability to relate mechanistic insights to human health, due to the high degree of molecular conservation and outstanding molecular, genetic, and genomic tools. In this study, we used *C. elegans* to fill the gap between very high-throughput *in vitro* systems that are hampered by low physiological and environmental relevance, and more physiologically complex organisms that offer more relevance to human and wildlife health, but less mechanistic power and lower throughput.

In this study, we tried to maximize these advantages of *C. elegans* by combining a comprehensive systems toxicology approach using toxicogenomics–proteomics and pathway analysis with functional genetics based on *C. elegans* mutant libraries. The functional genetic approach enhances and complements the predictive power of toxicogenomics–proteomics and pathway analysis, resulting in a more thorough investigation of the mechanism of toxicity of MWCNTs. The representative genes from each pathway detected through pathway analysis were selected, and the responses of their loss-of-function mutants upon exposure to MWCNTs were compared with that of *wildtype*. We interpreted the response of each mutant compared to *wildtype* as an indicator of how these genes and/or pathways get involved in the toxicity of MWCNTs. By linking molecular level response with higher level effects through multi-omics, and then applying bioinformatics and functional mutant analyses, we were able to identify genes and pathways that are involved in adverse outcomes after MWCNTs exposure. This approach will eventually be used to develop an "Adverse Outcome Pathway (AOP)", concept that has been recently introduced as a conceptual framework for the linking of multiple levels of biological organization, connecting an initial molecular event with an adverse outcome at a biological level of organization relevant to risk assessment [17].

We observed that the exposure to pristine MWCNT did not induce any mortality in *wildtype C. elegans*, up to 500 mg/L. Therefore, the multi-omics based mechanism study was conducted with pristine MWCNTs at that concentration, which brought about a 15% decrease of reproduction potential (1 mg/L), whereas hydroxylated MWCNT (OH-MWCNT) was used to identify rescue or exacerbated effects of functional mutants using mortality as endpoint. In fact, CNTs are often functionalized by hydrophilic ligands, as the commercial application of CNTs is often limited by their low solubility and dispersibility in organic or inorganic solutions [18]. To overcome this difficulty, the material surface was functionalized by introducing hydrophilic chemical groups, which lead to higher dispersibility while maintaining the unique properties of pristine CNTs [19]. Functionalized CNTs are therefore widely used as additives, catalysts, sensors, absorbents, intracellular carriers, electrodes, and imaging agents [20,21].

2. Materials and methods

2.1. Multi-wall carbon nanotube

Pristine and OH-MWCNTs were purchased from Cheaptube (www.cheaptube.com). Detailed physicochemical properties of pristine and OH-MWCNTs are presented in Table S1. Before treatment with *C. elegans*, each type of MWCNT was sonicated for 1 h (Branson-5210 sonicator) in distilled water (DW). From stock solutions, experimental concentrations of MWCNTs were prepared in K-media for *C. elegans* exposure. The shape and crystal structure of the MWCNTs were determined using a LIBRA 120 transmission electron microscope (TEM) (Carl Zeiss, Oberkochen, Baden-Württemberg, Germany). The size distribution and zeta potential of MWCNTs in *C. elegans* K-media (0.032 M KCl and 0.051 M NaCl) was measured using Electrophoretic Light Scattering Spectrophotometer (ELS-8000, Otsuka Electronics Co., Inc., Osaka, Japan) (Table S1). Hydrodynamic diameters (HDD) ranged from 700 to 1000 nm in K-media. HDD of OH-MWCNT (785.2 nm) was much smaller than that of pristine (1097.5 nm), however the zeta potentials which indicate the ionic stability in aquatic media were observed very similar, such as −30.93 mV for pristine and −31.47 mV for OH-MWCNT.

2.2. C. elegans and treatment of MWCNTs

C. elegans were grown in Petri dishes on nematode growth medium (NGM) and fed with OP50 strain *Escherichia coli*. Worms were incubated at 20 °C, with young adults (3 days old) from an age-synchronized culture and then used in all the experiments. *Wildtype* and mutants were provided by the *Caenorhabditis* Genetics Center (www.CGC.org) at the University of Minnesota. Detailed information on the mutant strains used in this study is presented in Table S2. Survival and reproduction test were performed on the *wildtype* after 48 h and 72 h exposure respectively, as described previously [22]. For microarray and proteomics analyses, *C. elegans* were exposed to 1 mg/L of the pristine MWCNT for 4 and 24 h and the total RNA and protein lysates were then prepared. *Wildtype* and mutant *C. elegans* were exposed to pristine and OH-MWCNTs at the concentration of 500 mg/L for *C. elegans* survival tests.

2.3. Microarray

Age synchronized young adult worms pooled samples were obtained for the exposure conditions at 0, 4 and 24 h, together with five control samples at 24 h. The total RNA from the exposed and control worms was prepared according to the standard protocol of the RNeasy Mini kit (Qiagen, Hilden, Germany). Five μg aliquots of each total RNA product were used for reverse and *in vitro* transcription followed by application to a GeneChip® *C. elegans* Genome Array (Affymetrix, Santa Clara, CA, USA), which contained 22,500 probe sets against 22,150 unique *C. elegans* transcripts. After the final wash & staining step, Affymetrix GeneChip® *C. elegans* Genome Array was scanned using Affymetrix Model 3000 G7 scanner and the image data was extracted through Affymetrix Command Console software v.1.1. Expression data were generated by Affymetrix Expression Console software v 1.1. For normalization, the RMA algorithm implemented in Affymetrix Expression Console software was used. Additionally, probe sets that were not called present by the MAS5 detection were filtered out. Two analyses of gene expression were performed. One analysis compared the treatment samples across time, whereas the other one compared the 24 h exposure condition with the 24 h controls. Details are presented in the following.

2.4. Ingenuity pathways analysis on the microarray data

A cutoff value of 1.5-fold was chosen to identify differentially expressed genes, which were given as input to Ingenuity Pathway Analysis (IPA) (Ingenuity Systems, http://www.ingenuity.com). For each gene within the cutoff value, their id number (probe #) and corresponding fold change was tabulated in Microsoft excel and imported into IPA (Ingenuity Systems), for canonical pathways analyses. The statistical significance of each pathway or gene list was determined by IPA using a Fisher Exact Test with threshold $p < 0.05$. IPA was also used to construct networks of interacting genes. IPA contains a database that uses the an up-to-date knowledge base available on genes, proteins,

chemicals, normal cellular and disease processes, and signaling and metabolic pathways needed for pathway construction.

2.5. Gene ontology analysis of microarray data at the 24 h exposure condition

Differentially expressed genes were identified by comparing the 24 h exposure sample with the five 24 h control samples (see Fig. S6 for the statistic used and its probability distribution). A combined criteria of p-value < 0.01 and fold change > 1.5 were used, following recommendations by the Microarray Quality Control Project [23]. Gene ontology categories were identified with AmiGo2 (http://amigo2.berkeleybop.org/), using a threshold of p-value < 0.05.

2.6. 2-DE and identification of DEPs by LC–MS/MS

Three samples of whole protein lysates were prepared from about 6000 pooled young adult *wildtype C. elegans*. For 2-DE analysis, 800 μg of the protein lysates were rehydrated in 18 cm IPG strips at pH 5.5–6.7, followed by isoelectrofocusing and 2-D separations onto 18% (v/v) homogenous SDS–polyacrylamide gels, according to the manufacturer's instructions (GE Healthcare). For protein identification, 2-D gel spots were digested with trypsin, and the resulting tryptic peptides were separated and analyzed using reversed phase capillary HPLC directly coupled to a Finnigan LCQ ion trap mass spectrometer (LC–MS/MS). The MS and MS/MS spectra of peptides eluted from the column were acquired and subjected to query the *C. elegans* subset database in NCBInr, using the MASCOT program (http://www.matrixscience.com) with the following parameters: oxidation (methionine), peptide mass tolerance at 2 Da, MS/MS ion mass tolerance at 1 Da, 2 missed cleavages, and charge states (+1, +2, and +3). The proteins identified with at least one significant peptide hit, as defined by a MASCOT probability analysis, were accepted.

2.7. Pathway analysis of the proteomics data

Given the small number of identified proteins, tests based on the relative over- or under-abundance of proteins in reference pathways, such as those implemented in IPA, were not able to detect any significantly affected pathways. For this reason, a method based on network analysis was developed and implemented in-house to analyze the proteomics results. The method was composed of four steps. First, a reference network was built using the *C. elegans* entries in the KEGG reference database. In this reference network, nodes represented *C. elegans* genes and links represented *C. elegans* pathways. Connectivity was thus defined by gene co-annotation, i.e., any pair of genes annotated to the same pathway were connected by a link, corresponding to the common pathway. Second, each detected protein was mapped (as a gene product) to the node of the network representing the corresponding gene. Third, affected pathways were identified by means of the shortest paths in the network which connected any two detected proteins and which consisted only of detected proteins. Each of those connecting shortest paths added 1 to a score which was tracked independently for each protein and each pathway. And fourth, statistical significance of the score obtained for each protein and each pathway was calculated by comparison with the distribution of scores corresponding to the null hypothesis, calculated by a bootstrap procedure with random sets of proteins. The main advantage of this approach, compared to the over-/under-abundance method mentioned above, resides in that it considers relationships between all genes on a genome-wide manner, as defined by pathway annotations, instead of considering pathways as isolated sets of genes.

The reference network for *C. elegans* built in the current study encompassed 1878 proteins connected by pathways from a total of 123 pathways. The shortest paths connecting the 22 detected proteins were searched with the standard Dijkstra's algorithm. The distribution of scores for the null case was calculated with 1000 random sets, each one generated by simple random sampling of 22 proteins from the complete set of 1878 proteins. A value of $p < 0.01$ was used as threshold of statistical significance for the resulting p-values.

Two additional variations of this basic procedure were implemented to perform further analyses: a probabilistic approach and an ortholog-based approach. In the probabilistic analysis, proteomics results were interpreted in a probabilistic way. Each detected protein was assigned a probability of $(1 - p)$, with $0 < p \ll 1$, whereas each undetected protein was assigned a probability of p, with a chosen value of $p = 0.1$. As a consequence, all shortest paths in the reference network were evaluated by multiplying the obtained probabilities of the nodes (proteins) in the path. The resulting number was added to the score of the proteins and pathways in the shortest path. It should be noted how this procedure generalized the basic approach presented above, which corresponded to $p = 0$. Notice also that conclusions from this probabilistic version of the analysis are by construction more speculative, aiming at generating hypothesis and uncovering possible targets for additional experiments. On the other hand, in the ortholog-based approach, the reference network was built with the general reference pathway of KEGG based on orthologs, instead of the specific genes and pathways of *C. elegans*. In this case, the crucial aspect is the homology between *C. elegans* genes/proteins and KEGG orthologs. This second variation of the analysis tries to exploit known relationships between orthologs, which may be important for the problem under study but that have not been identified or annotated for the target species.

2.8. Quantitative real time-polymerase chain reaction

For quantitative real time-polymerase chain reaction (qRT-PCR) analysis, worms were exposed to pristine and OH-MWCNTs for 24 h, and gene expression was analyzed using IQTM SYBR Green SuperMix (Bio-Rad). Quantitative RT-PCR was carried out on selected genes using a Chromo4 Real-Time PCR detection system (Bio-Rad). The primers were constructed based on sequences retrieved from the *C. elegans* database (www.wormbase.org) and described in Table S3. qRT-PCR conditions were optimized and efficiency and sensitivity tests were performed for each gene prior to the main experiment. Three biological replicates were conducted for each qRT-PCR analysis.

2.9. Statistical analysis

Data relating to survival and reproduction were presented in arbitrary units compared to the control, with statistical differences between the *wildtype* and mutants being determined by an analysis of variance (ANOVA) and Dunnett's multiple comparison test. For the expression of genes, data were presented as mean value compared to control, and statistical analysis was conducted using the two-tailed t-test. All statistical tests were performed with the Statistical Package for Social Sciences 12.0 KO (SPSS Inc., Chicago, IL, USA).

3. Results and discussions

To gain a comprehensive insight of toxic mode of action of MWCNTs to *C. elegans*, multi-omics analyses (i.e. transcriptomics and proteomics) were conducted for *C. elegans* exposed to pristine

MWCNT. The exposure concentration for omics analysis was selected based on the organismal response of *C. elegans*, such as, survival and reproduction (Fig. S1). No increased mortality was observed for *C. elegans* after to 500 mg/L of MWCNT, whereas the reproductive potential was decreased by about 15% after exposure to 1 mg/L of MWCNT for 72 h. Hence, we selected 1 mg/L as an exposure concentration for both omics studies, with investigations centering on mortality for OH-MWCNT, and reproductive potential for pristine MWCNT. We conducted both microarray and proteomic analyses at 4 and 24 h after exposure to pristine MWCNT, with the aim of gaining an insight into transcriptional–translational regulation. We expected that the protein level response of later time point (24 h) would reflect transcriptional response of earlier time point (4 h).

3.1. Microarray and pathway analysis

The microarray data were submitted to the Gene Expression Omnibus database (GEO accession No. GSE24847). The analysis of 4 and 24 h exposure condition compared with 0 h demonstrates that a greater degree of regulation of the transcriptome had occurred at 24 h than at 4 h. The number of differentially expressed genes (DEGs) in *C. elegans* exposed to MWCNTs for 24 h was more than twice that after 4 h exposure, as 2247 genes vs. 846, (Fig. 1A). Down-regulated DEGs were more important than up-regulated ones at both time points (Fig. 1B). The full list of DEGs is presented in Table S4.

Although some transcripts were commonly regulated at both time points, a large number of transcripts were differentially regulated at each exposure condition (Fig. 1). About 31% of the DEGs after 24 h exposure overlapped those after 4 h exposure, whereas about 72% of DEGs after 4 h exposure overlapped those after 24 h exposure. This is indicative of the continuation of early biological responses up to 24 h as well as the development of additional stress responses when exposure is maintained.

In a recently conducted microarray study of *C. elegans* exposed to amide-single wall carbon nanotube (SWCNT) [24], 14 up- and 2085 down-regulated genes were reported after exposure to L1 stage *C. elegans* at 500 mg/L for 48 h. In our study, 983 up-and 1267 down-regulated genes were observed for young adults exposed to 1 mg/L for 24 h. It is difficult to compare microarray result from independent experiments, as differences in DEGs may be influenced by differences in the specific biological systems, array platforms and statistical methods. The number of up-regulated genes was much higher in our study as compared to that in the SWCNT study [24], which may be due to the fact that our exposure conditions reflected a relatively mild stress response, whereas the exposure conditions of the SWCNT study induced a much more severe stress responses, which was more likely to lead to transcriptional shut-down. As the value of realistic exposure scenarios is increasingly recognized within nano-toxicity studies, our results will have substantial relevance to future CNT environmental toxicity studies.

In our study, worms exposed to MWCNTs for the longer time (24 h) showed stronger transcriptomal response than for the shorter time (4 h). However, in another ecotoxicogenomics study of the single cell green alga, *Chlamydomonas reinhardtii*, a shorter exposure time (15 min) resulted in a stronger transcriptomal response than the longer exposure time (1 h), upon exposure to silver nanoparticles (AgNPs). While that study was conducted using a single cell model with AgNPs, as opposed to MWCNTs, it is interesting to note the reduced response of *C. reinhardtii* at the later time point, indicating the cell's adaptive response at the transcriptome level [25]. It is also interesting to note that in this transcriptomics analysis the exposure effects are observed compounded with the physiological changes across time.

Genome-wide expression analysis, followed by integrated bioinformatics tools, was used to identify interacting gene networks which are likely to be critical for a full understanding of the mechanism of toxicity. To better understand the mechanism of toxicity, we performed IPA on both 4 and 24 h data sets of DEGs from the microarray analysis. The networks (Fig. S2) and canonical pathways (Table 1), which indicate the key biological pathways and the molecular relationships between genes/gene products modulated by MWCNT exposure, were generated from DEGs of microarray analysis. Eukaryotic initiation factors 2 (eIF2), eIF3, eIF4 and AKT were major connecting molecules in the network generated with DEGs from 4 h MWCNT exposure (Fig. S2A) while pro-inflammatory transcription factor, NF-κB was shown to be connected to the majority of molecules in the network generated with DEGs after 24 h MWCNT exposure. While NF-κB is absent in the *C. elegans* genome (Fig. S2B), which is certainly due to the fact that the IPA database is mainly built from human and mouse databases revealing a clear limitation in the application of this software to organisms different from humans and mice. This result, however, implies that the functional counterpart of NF-κB genes and related networks in *C. elegans*, which is as yet unknown, may be involved in MWCNT toxicity [26,27]. Indeed, the involvement of inflammation, including NF-κB activation, has frequently been observed in previous CNT toxicity studies using both mammalian *in vivo* and *in vitro* models [28–30]. Gene pathways, such as xenobiotic metabolism signaling, fatty acid metabolism, mammalian target of rapamycin (mTOR) and extracellular signal-regulated kinases/mitogen-activated protein kinase (ERK/MAPK) signaling pathways were also observed to be significantly changed in *C. elegans* exposed to MWCNTs (Table 1). Xenobiotic metabolism, mTOR and MAPK pathway are well known

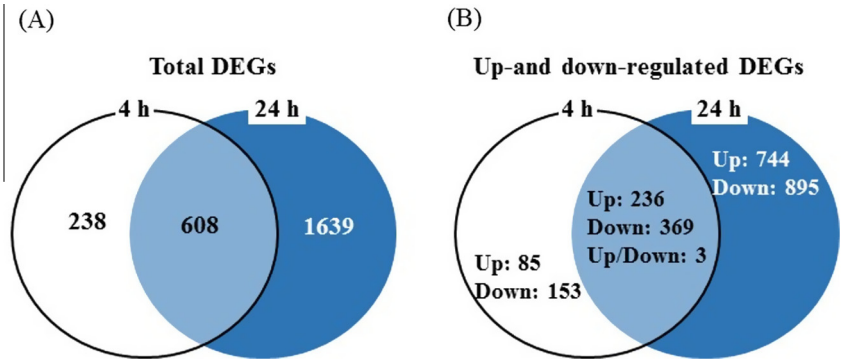

Fig. 1. Numbers of differentially expressed genes (DEG) by 4 and 24 h pristine MWCNT exposure in *C. elegans* based on microarray experiment. Venn diagram illustrated the overlap between 4 and 24 h DEGs on exposure to pristine MWCNT.

Table 1
Top canonical pathways from ingenuity pathways analysis using differentially expressed genes by 4 and 24 h pristine MWCNT exposures.

Canonical pathways	No. of genes	*p*-value	Ratio
4 h			
Xenobiotic metabolism signaling	18	8.1×10^{-4}	0.06
LPS/IL-1 mediated inhibition of RXR function	17	2.5×10^{-6}	0.077
Fatty acid metabolism	15	9.04×10^{-5}	0.077
Tryptophan metabolism	14	2.47×10^{-3}	0.055
Regulation of eIF4 and P70S6K signaling	13	4.61×10^{-3}	0.096
eIF2 signaling	13	1.33×10^{-3}	0.125
mTOR signaling	13	1.25×10^{-2}	0.079
ERK/MAPK signaling	13	2.08×10^{-2}	0.064
Valine leucine and isoleucine degradation	12	8.5×10^{-3}	0.108
Propanoate metabolism	11	6.48×10^{-3}	0.085
24 h			
LPS/IL-1 mediated inhibition of RXR function	21	1.13×10^{-2}	0.095
Fatty acid metabolism	21	1.67×10^{-2}	0.107
Bile acid biosynthesis	10	3.45×10^{-2}	0.093
Glutamate receptor signaling	9	1.89×10^{-2}	0.129
Cardiomyocyte differentiation via BMP receptors	4	1.89×10^{-2}	0.2

to be activated by a wide range of xenobiotics and those pathways are known to be conserved from *C. elegans* to humans [31,32].

Additionally we conducted Gene Ontology (GO) analysis of the DEGs by comparing the 24 h exposure condition and with the 24 h controls (GEO accession Nos. GSE14932 and GSE23013) (Tables 2 and S6) using AmiGO2 (amigo2.berkeleybop.org/). In total, 54 Biological progress (BP) GO terms, 18 Cellular component (CC) GO terms and 20 Molecular function (MF) GO terms were enriched (Table S6). Biological processes for down-regulated genes were related to metabolic process such as 'primary metabolic process' (GO:0044238) and 'cellular metabolic process' (GO:0044237), whereas many of up-regulated genes belong to the related reproductive development such as 'embryo development ending in birth or egg hatching' (GO:0009792), 'female gamete generation' (GO:0007292) and 'germ cell development' (GO:0007281). Similarly, a few of recent studies documented that nanomaterials, such as gold, silver, and gold-silver alloy nanoparticles were shown to have reproductive toxicity by impairing key sperm functions, somatic and reproductive cells, and mammalian gametes [33–35]. The results of GO analysis suggest that exposure MWCNTs may contribute to reduce reproduction potential. Moreover, two GO terms, 'phagosome–lysosome fusion involved in apoptotic cell' (GO:0090389) and 'phagolysosome assembly' (GO:0001845) were found to be enriched in the group of up-regulated genes, which was not found from IPA analysis. This finding from GO analysis indicated that phagocytosis could be a potential uptake mechanisms of MWCNTs.

3.2. Proteomics and pathway analysis

Proteomics analysis was subsequently conducted, using 2-D electrophoresis, on *C. elegans* which were exposed to the same conditions, which revealed 45 differentially expressed spots by MWCNT exposure (Fig. S3). The TurboSEQUEST program (Table 3) identified 22 proteins (11 increased and 11 decreased proteins compared to control values). The identification of differentially expressed 2-D gel spots using LC–MS/MS revealed that actin proteins (act-2,-3,-4,-5) were most commonly increased due to MWCNT exposure, whereas heat shock proteins (hsp-4,-70), phosphoethanolamine methyltransferase (pmt-2), malate dehydrogenase (mdh-1), GABA transaminase (gta-1) and aspartyl protease (asp-1) were decreased.

Pathway analysis of the proteomics data was thoroughly performed using in-house software with the three versions of the proposed network approach: basic, probabilistic and ortholog-based (see details in Methods section). Results are shown in Table 4. The basic version of the analysis detected the Phagosome as an affected pathway, together with greatly over-expressed actin proteins (spots IN19 and IN20 in Table 3). Note that the three network approach yielded not only significantly affected pathways but also the relevant proteins. Probabilistic analysis revealed the involvement of the citrate acid cycle and oxidative phosphorylation pathway, together with an F-type ATPase subunit, H28O16.1, a protein greatly under-expressed in the 2D gel (spot DE12 in Table 3). This protein is related to many V-type ATPases subunits, which are components of vacuolar ATPases which pump protons in lysosomes. Considering the close relationship between the endosome, phagosome and lysosome pathways, results from pathway analyses, both basic and probabilistic, suggest the uptake and subsequent toxic events of MWCNTs in *C. elegans*. The role of the citrate acid cycle in response to SWCNT has been recently reported for *C. elegans* [24]. These authors related this to oxidative stress based on the evidence of decreased expression of the mitochondrial sod gene, *sod-3*. We also found increased sensitivity of the *sod-3* mutant to MWCNT, as discussed below.

The third version of the pathway analysis, based on KEGG orthologs instead of the actual *C. elegans* genes or proteins, also detected the phagosome pathway, as in the other two analyses,

Table 2
The representative gene ontology (GO) term enriched for DEGs by comparing 24 h pristine MWCNT exposure with control using AmiGo2 (http://amigo2.berkeleybop.org/) (*p*-value < 0.05).

GO BP ID	Term	*p*-value	Odds ratio	ExpCount	Count	Size
GO:0044238	Primary metabolic process	0.013	0.358	12	6	3099
GO:0044237	Cellular metabolic process	0.035	0.422	11	6	2807
GO:0007292	Female gamete generation	0.013	4.858	1	4	235
GO:0009792	Embryo development ending in birth or egg hatching	0.013	2.411	10	16	2436
GO:0007281	Germ cell development	0.035	3.557	1	4	316
GO:0090389	Phagosome–lysosome fusion involved in apoptotic cell clearance	0.016	86.460	0	1	4
GO:0001845	Phagolysosome assembly	0.035	32.401	0	1	9

Table 3
Differentially expressed proteins by pristine MWCNT exposure identified using TurboSequest software.

Spot ID	Sum of mascot score	No. of identified peptide	Protein MW/pI value	% Coverage	Accession number	Protein name	Identified peptide sequence
DE4	53	3	72244/5.03	5	gi|17534771	Heat Shock Protein family member (hsp-4)	K.NQLTINPENTIFDAK.R
DE12	88	3	57752/8.98	8	gi|71988063	Hypothetical protein H28O16.1	R.EVAAFAQFGSDLDASTQQLLNR.G
DE18	222	17	49738/5.61	42	gi|17561380	Phosphoethanolamine MethylTransferase family member (pmt-2)	R.NADVLIFNNALSQIITNADLLTDFLK.N
DE18	52	1	37943/5.80	3	gi|193202489	Hypothetical protein D2092.6	K.SSEEIIIEEK.E
DE21	150	10	35098/9.39	31	gi|17554310	Malate DeHydrogenase family member (mdh-1)	R.IQDAGTEVVNAK.A
DE5	409	13	72244/5.03	21	gi|17534771	Heat Shock Protein family member (hsp-4)	K.KTDVHEIVLVGGSTR.I
DE5	190	9	53022/8.67	13	gi|17541228	GABA TransAminase family member (gta-1)	R.TDFADGISHALTSIAPK.G
DE5	147	6	42666/5.81	16	gi|25151802	ASpartyl Protease family member (asp-1)	K.TQPDLIFTIGGAQFPVK.S
DE5	132	4	69781/5.26	6	gi|156352	Heat shock protein 70A	R.IINEPTAAAIAYGLDK.K
DE5	117	3	70396/5.42	4	gi|17507981	Heat Shock Protein family member (hsp-70)	R.IINEPTAAALAYGLDK.G
DE5	52	2	33806/6.50	8	gi|7494627	Heat shock protein 70 homolog – *C. elegans*	K.VEIIANDQGNR.T
IN7	226	12	53022/8.67	20	gi|17541228	GABA TransAminase family member (gta-1)	K.AVQTMLCGTSANENAIK.T
IN8	103	5	39713/9.02	16	gi|498329	uses second of two potential start sites	R.VAQNPADLAELPEEK.I
IN19	376	26	41638/5.30	59	gi|14278147	Chain A, crystal structure of *C. elegans* Mg-Atp actin complexed with human gelsolin segment 1 at 1.75 A resolution	K.LCYVALDFEQEMATAASSSSLEK.S
IN19	375	25	40400/5.56	61	gi|71994099	ACTin family member (act-4)	K.LCYVALDFEQEMATAASSSSLEK.S
IN19	179	17	41846/5.44	25	gi|17551718	ACTin family member (act-5)	M.EEEIAALVVDNGSGMCK.A
IN19	86	7	9247/4.91	77	gi|552061	Actin	R.AVFPSIVGRPR.H
IN20	211	17	41769/5.30	52	gi|17563820	ACTin family member (act-3)	K.SYELPDGQVITVGNER.F
IN20	211	17	41751/5.30	52	gi|17568985	ACTin family member (act-4)	K.SYELPDGQVITVGNER.F
IN20	211	17	41751/5.29	54	gi|17557190	ACTin family member (act-2)	K.SYELPDGQVITVGNER.F
IN20	203	16	37255/5.37	52	gi|17568987	ACTin family member (act-4)	K.SYELPDGQVITVGNER.F
IN20	68	8	41846/5.44	22	gi|17551718	ACTin family member (act-5)	M.EEEIAALVVDNGSGMCK.A

together with several pathways concerning actin-related cellular processes, infection diseases and cardiomyopathies (Table 4). Remarkably, the list of relevant proteins revealed just one additional protein, the heat shock protein-70 (HSP-70), which is present because of its annotation to the Influenza A pathway. Examination of this pathway revealed that hsp-70 is, in this context, related to endosome function [36–38]. However, this relationship has not been observed for *C. elegans*, and as such, is as of yet hypothetical. In any case, this protein appeared to be clearly under-expressed in the proteomics assay and the suggested endocytosis reinforces the detection of phagocytosis by the two other versions of the analysis. In addition, the protein hsp-4 was highly under expressed (spot DE4 in Table 3). Hsp-70s were also part of DEPs by MWCNTs, which may also imply that the relationship between the endosome and hsp proteins also holds for *C. elegans*. As hsp-4 was down-regulated at both gene and protein levels (Table S5), which may also imply the involvement of endoplasmic reticulum (ER) stress in *C. elegans* upon exposure to MWCNTs as discussed below. In summary, the three pathway analyses performed on the set of detected proteins highlighted phagocytosis as an affected pathway and also suggested the role of endocytosis and ER stress in the uptake and toxicity of MWCNT.

3.3. Transcriptomics–proteomics

To investigate the possibility of a relationship between the transcriptional and translational responses to MWCNTs toxicity, DEPs from proteomics were compared with DEGs obtained from microarray analysis (Table S5). Table S5 shows that 7 proteins or protein domains were differentially expressed in both proteomics and transcriptomics assays. Among those 7 gene/proteins, *pmt-2*, *mdh-1*, *hsp-4* and *hsp-70* were under-expressed at both transcriptional and translational levels. In the other 3 cases, *gta-1*, *asp-1* and *act-2,3,4,5*, the transcriptional and translational levels are modified in opposite directions. Unfortunately, due to the small number of proteins, the observed degree of matching or mismatching cannot be considered as statistically significant. In any case, low matching between transcriptomics and proteomics results has been frequently found, as various cellular processes other than direct transcriptomic–proteomic level regulation (i.e., post-transcriptional and post-translational regulations, complex regulatory loops), may arise due to toxicity and chemical response in organisms [39,40]. A similar case was also identified in a recently conducted ecotoxicogenomic study of AgNPs- exposed *C. reinhardtii* [25], where the authors interpreted mRNA abundance

Table 4
List of pathways and proteins detected by the network analysis conducted on differentially expressed proteins.

	Pathway (KEGG ID)	Protein (KEGG id)
Basic	Phagosome (cel04145)	ACT-2 (CELE_T04C12.5) ACT-3 (CELE_T04C12.4) ACT-4 (CELE_M03F4.2)
Probabilistic	Phagosome (cel04145)	ACT-2 (CELE_T04C12.5) ACT-3 (CELE_T04C12.4) ACT-4 (CELE_M03F4.2)
	Citrate cycle (TCA cycle) (cel00020)	MDH-2 (CELE_F20H11.3)
	Oxidative phosphorylation (cel00190)	H28O16.1 (CELE_H28O16.1)
Ortholog-based	Influenza A (ko05164)	ACT-2 (CELE_T04C12.5) ACT-3 (CELE_T04C12.4) ACT-4 (CELE_M03F4.2) HSP-70 (CELE_C12C8.1)
	Phagosome (ko04145)	ACT-2 (CELE_T04C12.5) ACT-3 (CELE_T04C12.4) ACT-4 (CELE_M03F4.2)
	Regulation of actin cytoskeleton (ko04810)	ACT-2 (CELE_T04C12.5)
	Focal adhesion (ko04510)	ACT-3 (CELE_T04C12.4)
	Adherens junction (ko04520)	ACT-4 (CELE_M03F4.2)
	Tight junction (ko04530)	
	Bacterial invasion of epithelial cells (ko05100)	ACT-2 (CELE_T04C12.5)
	Vibrio cholerae infection (ko05110)	ACT-3 (CELE_T04C12.4)
	Pathogenic Escherichia coli infection (ko05130)	ACT-4 (CELE_M03F4.2)
	Shigellosis (ko05131)	
	Salmonella infection (ko05132)	
	Hypertrophic cardiomyopathy (HCM) (ko05410)	ACT-2 (CELE_T04C12.5)
	Arrhythmogenic right ventricular cardiomyopathy (ARVC) (ko05412)	ACT-3 (CELE_T04C12.4)
	Dilated cardiomyopathy (ko05414)	ACT-4 (CELE_M03F4.2)
	Viral myocarditis (ko05416)	
	Leukocyte transendothelial migration (ko04670)	ACT-2 (CELE_T04C12.5)
	Phototransduction – fly (ko04745)	ACT-3 (CELE_T04C12.4) ACT-4 (CELE_M03F4.2)

to be a good indicator of the presence of a protein, but not sufficient to explain the variation in protein quantities. However, such a discrepancy between transcriptome and proteome level responses may also suggest that only a few of the affected genes have functional consequences and that the alteration of the majority of genes may be due to homeostatic responses, which have little toxicological relevance. Another possible explanation may lie in the time delay between transcription and translational response. It should be noted that we designed the same exposure concentrations and durations for both transcriptomics and proteomics analyses. The proteins eIFs were the major connecting molecules in the network generated with DEGs from 4 h MWCNT exposure (Fig. S2A). Since these proteins are involved in the initiation phase of eukaryotic translation, their up-regulation by MWCNTs suggests an increased overall translation rate in defense against MWCNT insult. A remarkable point is the contrast between the very large over-expression of actin proteins (×85.38) compared to the under-expression of the corresponding mRNA (×0.305). This suggests a strong disturbance to the regulation of actin proteins in the cytoplasm, as a result of the uptake of MWCNT.

The uptake of MWCNTs by phagocytic mechanism has been previously reported [41,42]. In this study, phagocytosis was found in both transcriptomics (Table 2, phagosome–lysosome fusion involved in apoptotic cell (GO:0090389) and phagolysosome assembly (GO:0001845)) and proteomics (pathway analysis: Table 4, Phagosome (cel04145)). This finding strongly suggests phagocytosis as a major mechanism of MWCNTs uptake.

3.4. Validation of hypothesis using C. elegans functional mutants

Combining the results from the pathway analyses, we found phagocytosis, and more speculatively, endocytosis, ER stress and oxidative stress as potential mechanisms of uptake and toxicity for MWCNTs in *C. elegans*. To validate these hypotheses, we selected the genes on those pathways and we examined the response of the loss-of-function mutants for those genes. They were *ced-10(n3246)*, *dyn-1(ky51)* and *rab-7(ok511)* for phagocytosis, *rme-1(b1045)*, *−2(b1008)*, and *−8(b1023)* for endocytosis, and *hsp-4(ok514)* for ER stress response. Oxidative stress response was examined with antioxidant enzymes genes, *sod-3(gk235)* and *ctl-2(ok1137)*, as well as, genes in oxidative stress response signaling, such as, *pmk-1(km25)*, *daf-16(mu86)* and *cep-1(gk138)*.

We tested these multi-omics-driven hypotheses using pristine MWCNTs, however, pristine MWCNT did not affect any of the tested mutants or *wildtype*, up to 500 mg/L, we therefore further examined the response of OH-MWCNT. Functionalized CNTs are generally considered to be more biocompatible than pristine CNTs due to their improved hydrophilicity and dispersion in biological media [43,44]. Although surface hydrophilicity of MWCNTs could alter their cell uptake, the effect of hydrophilicity on their toxicity is not clearly understood [45]. In this study, our results show that OH-MWCNT exposure leads to a decrease of worms' survival in about 60% (Fig. S4). This can be attributed to the increased dispersion of hydroxylated MWCNTs in test media facilitating uptake and toxicity.

3.4.1. Uptake: phagocytosis and endocytosis

The uptake of nanomaterials *via* ingestion, and the subsequent translocation into intestinal and reproductive cells has already been observed in *C. elegans* for a variety of NPs reviewed in Zhao et al. [46]. Here, we tested whether ingestion is the main route of uptake of MWCNTs, using a pharyngeal pumping defective mutant (*eat-2(ad465)*). We found that the toxicity was completely rescued in the *eat-2* mutant, which strongly suggests ingestion to be the main route of MWCNT uptake (Fig. S4). Many studies have demonstrated endocytosis/phagocytosis as the cellular uptake

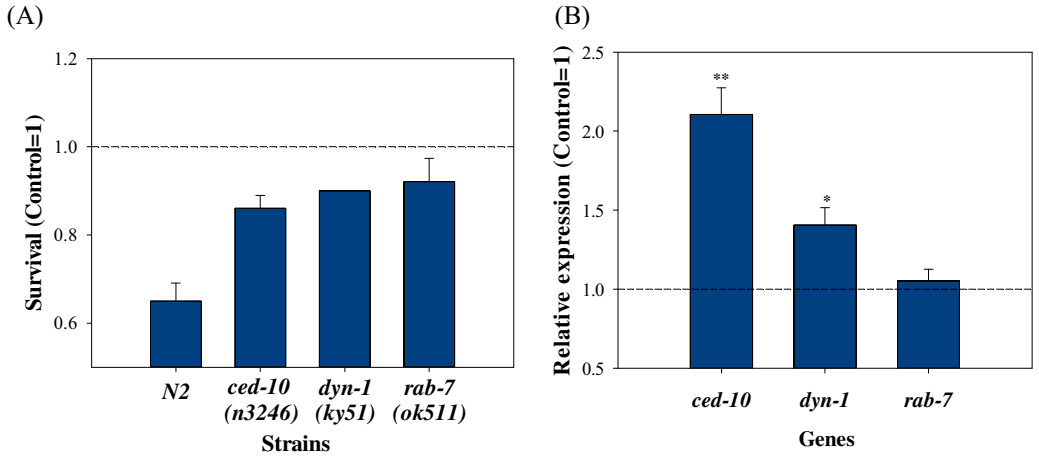

Fig. 2. Effect of phagocytosis on *C. elegans* by MWCNTs. Survival was conducted on *wildtype(N2)* and phagocytosis defective mutants *C. elegans* (*ced-10(n3246)*, *dyn-1(ky51)* and *rab-7(ok511)*) exposed to OH-MWCNT (A). The expression of *ced-10*, *dyn-1* and *rab-7* genes in *wildtype(N2)* exposed to OH-MWCNT using qRT-PCR (B). The results were expressed as the mean value compared to control (control = 1, $n = 3$; mean ± standard error of the mean; two-tailed *t*-test, $^{*}p < 0.05$, $^{**}p < 0.01$).

mechanism of CNTs [47–51], while others refer to endocytosis -independent internalization of CNTs [52,53]. Defective endocytosis was proposed as a toxic mechanism of amide-SWCNT in *C. elegans* [24]. The authors reported that amide-SWCNT inhibited endocytosis may result in the decreased growth *C. elegans* due to reduced nutrient uptake.

As the overall degree of evidence for ingestion and phagocytosis was stronger than that for the other functions, as determined through pathway analyses from proteomics and GO analysis from transcriptomics (Tables 2 and S6), we paid special attention to phagocytosis. Phagocytosis related genes from GO analysis, *lst-4* and *psr-1*, which are known to interact and activate the *dyn-1*, *rab-7* and ced-*10* genes. Thus we investigated the expression of the genes *dyn-1*, *rab-7* and ced-*10*. It has been known that CED-10 leads to the cytoskeleton reorganization necessary for engulfment [54–57], RAB-7 regulates the change of early into late endosomes, as well as their subsequent trafficking and fusion to lysosomes [58,59], and finally, DYN-1 is required for the efficient recruitment and fusion of endosomes and lysosomes to phagosomes, and hence, is critical to related toxic pathways [60,61]. OH-MWCNT-induced mortality was significantly rescued in all the phagocytosis defective mutants tested: *ced-10(n3246)*, *dyn-1(ky51)* and *rab-7(ok511)* (Fig. 2A). Subsequently, the expression of *ced-10* and *dyn-1* genes was increased about 2 and 1.5-fold compared to the control in response to OH-MWCNT exposure, whereas no alteration of *rab-7* gene expression was observed (Fig. 2B). While the specific reason for the non-alteration of *rad-7* gene expression remains to be elucidated, both mutant and gene expression results suggest that phagocytosis is one of the uptake mechanisms of MWCNT, directly affecting its toxicity to *C. elegans*.

As shown in Table 1, IPA revealed the mTOR pathway to be one of the top canonical pathways from 4 h DEGs. The mTOR pathway is the most reported and actively studied pathway, being known to co-ordinate autophagy and phagocytosis, and is closely related to the mechanistic steps of autophagy, as reviewed by Peynshaert et al. [62]. During autophagy, a phagophore is created which elongates into a double membrane autophagosome, while sequestering cytoplasmic material. This autophagosome can then fuse with a lysosome, resulting in an autolysosome [62]. Hence, the identification of the mTOR pathway as a major canonical pathway provides another line of evidence that phagocytosis is involved in the uptake of MWCNTs in *C. elegans*.

As described earlier in Section 3.2, the endocytosis pathway was detected in pathway analysis with the response of actin proteins. Hence, we therefore also investigated endocytosis using functional mutants on OH-MWCNT. The selected endocytosis genes were *rme-1*, which is associated with the promotion of molecule recycling from endosomes back to the cell surface [63], *rme-2*, a member of the lipoprotein receptor family, which is essential for yolk endocytosis [64], and *rme-8*, which is required for receptor-mediated and fluid-phase endocytosis and is essential for the development and viability of *C. elegans* [65]. Genetic inhibitors did not rescue OH-MWCNTs-induced toxicity, suggesting that endocytosis may not be a major uptake mechanism by MWCNT (Fig. 3A). On the contrary, increased sensitivity of the *rme-8(b1023)* mutant (Fig. 3A) and increased *rme-8* gene expression were concomitantly observed, which may suggest *rme* mutant affect MWCNT toxicity in a different way (Fig. 3B). Indeed, in addition to endocytosis, *rmes* are also known to be involved in development and reproduction [64,66] and the sensitive response of *rme* mutants might reflect this reproduction related pathway. We also found that pristine MWCNTs caused reproductive toxicity at a relatively low concentration (1 mg/L), whereas no mortality was observed in the *wildtype* up to a significantly higher concentration of 500 mg/L (Fig. S1). To further check whether *rmes* is involved in the reproductive toxicity of MWCNTs, we investigated the reproductive potential of MWCNTs in *rme* mutants and compared their responses with that of *wildtype* (Fig. 3C). The decreased reproduction potential by OH-MWCNT was rescued in the *rme-8* mutant, suggesting the involvement of the *rme* pathway in OH-MWCNT-induced reproduction toxicity. However, further investigation is needed to fully understand the response of *rmes* to the uptake and toxicity of MWCNTs in *C. elegans*.

3.4.2. ER stress and oxidative stress

The involvement of ER stress as a mechanism of toxicity of nanomaterials has been previously reported for silver nanoparticle-exposed human cells and for *C. elegans* exposed to gold nanoparticles [67,68]. However, no study so far has reported the involvement of ER stress as a mechanism of CNT toxicity. In this study, several lines of evidence indicate the involvement of ER stress in MWCNT toxicity. The ER stress indicator protein, HSP-4, was highly down-regulated as shown in DEGs and DEPs lists (Table S5). Furthermore, eIF2 signaling was observed in IPA conducted on microarray analysis (Fig. S2). The ER resident kinase, PERK-dependent phosphorylation of eIF2α, is one component of the Unfolded Protein Response (UPR), a coordinated program that promotes cell survival under conditions of ER stress [69,70].

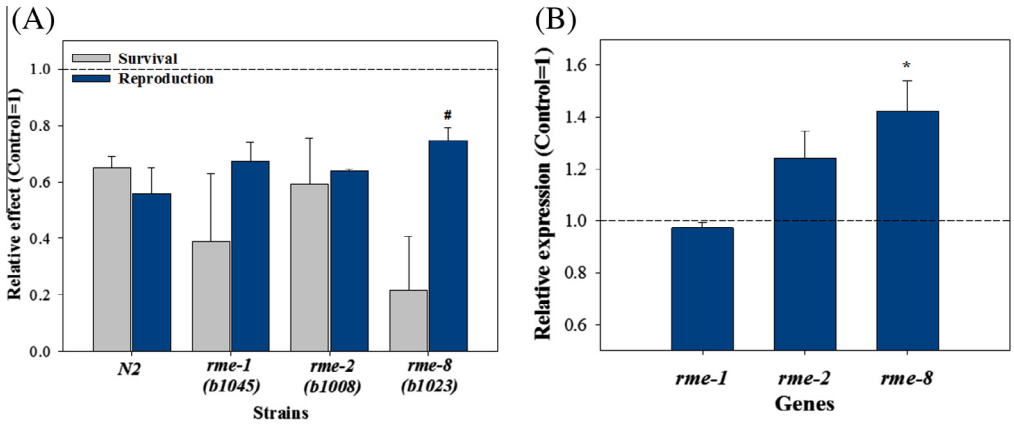

Fig. 3. Effect of endocytosis on *C. elegans* by MWCNT. Survival and reproduction analysis were conducted on *wildtype(N2)* and endocytosis defective mutants (*rme-1(b1045)*, *rme-2(b1008)* and *rme-3(b1023)*) *C. elegans* exposed to OH-MWCNTs (A). The expression of *rme-1*, *rme-2* and *rme-8* genes were measured in *wildtype(N2)* exposed to OH-MWCNT using qRT-PCR (B). The results were expressed as the mean value compared to control (control = 1, $n = 3$; mean ± standard error of the mean; two-tailed *t*-test, $^{*}p < 0.05$). The statistical difference between *wildtype* and mutants was also analyzed ($^{\#}p < 0.05$).

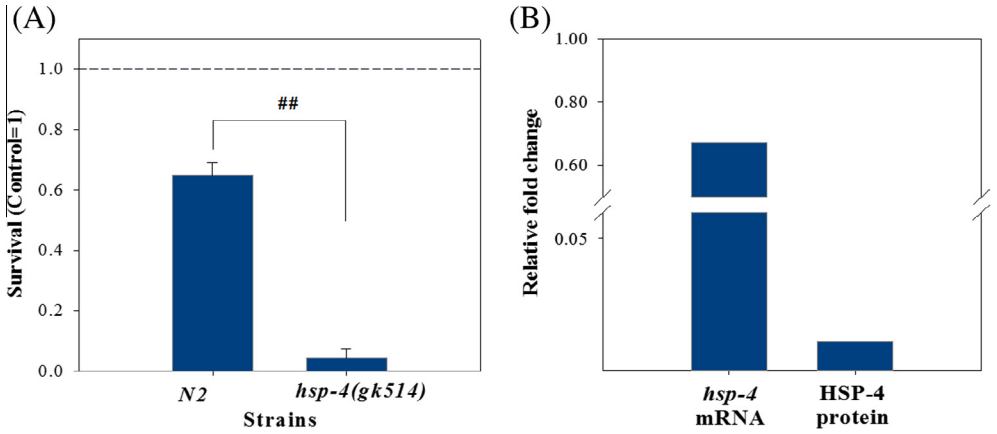

Fig. 4. ER stress of MWCNT in *C. elegans*. Survival was conducted on *wildtype(N2)* and *hsp-4(gk514)* mutant *C. elegans* exposed to OH-MWCNT (A). The results are expressed as the mean value compared to control (control = 1, $n = 3$; mean ± standard error of the mean). The statistical difference between *wildtype* and mutant was also analyzed ($^{\#\#}p < 0.01$). The expression of heat shock protein (hsp-4) in mRNA and protein level (B). Fold changes of mRNA and protein level were measured by microarray and proteomics.

Taking into account the role of eIF in ER stress may offer further evidence for a role of ER stress in MWCNT toxicity in *C. elegans*. Such growing evidence for the important role of ER in cellular stress response and cross talk between ER stress and oxidative stress, which is considered a main toxicity mechanism of MWCNTs [71,72], warrants further investigation of the involvement of ER stress in MWCNT toxicity.

The response of the *hsp-4(gk514)* mutant upon OH-MWCNTs exposure was examined, and a significantly increased sensitivity of *hsp-4* was found compared to that of *wildtype* (Fig. 4A), indicating the direct inducement of ER stress by MWCNTs. However, in this study, we found that the expression of *hsp-4* was down-regulated at both gene and protein levels (Fig. 4B and Table S5). Therefore, these results suggest that MWCNT exposure may affect the response of *C. elegans* toward ER stress, rather than directly initiating ER stress itself.

Oxidative stress followed by inflammation is considered to be the main mechanism of CNT toxicity [9,73–75]. However, a recent study on SWCNT toxicity in *C. elegans* reported that oxidative stress is not involved in SWCNT toxicity [24]. The decrease in *sod-3* gene expression was attributed to oxidative phosphorylation resulting from the decreased activity of the citrate cycle. In the current study, however, *sod-3*, *pmk-1* and *cep-1* mutants exhibited an increased sensitivity to OH-MWCNTs compared to that of the *wildtype*. This increased sensitivity was greatest for *pmk-1*, which exhibited an increased sensitivity of about 70% compared to the *wildtype* (Fig. S5). These mutant responses suggest that oxidative stress is also involved in OH-MWCNT-induced toxicity in *C. elegans*. Collectively, we found that each mutant exhibited a different sensitivity to MWCNT, although we cannot yet fully explain the variable responses of different mutants. Further investigation is needed in order to fully understand the mechanisms of uptake and toxicity of MWCNTs.

To conclude, the transcriptomics, proteomics and subsequently functional genetic analysis provided detailed insights into the mechanisms of uptake and toxicity in *C. elegans* exposed to MWCNTs. From the detailed analysis of the functional networks of *C. elegans*, we can derive phagocytosis, endocytosis, ER stress and oxidative stress as mechanisms of uptake and toxicity for MWCNTs in *C. elegans*. The power of network-based approaches for pathway analysis is remarkable, especially concerning the generation of hypotheses which are sufficient for the guidance of further experimental studies. The integrated systems toxicology approach applied in this study provided a comprehensive insight into the toxicity of chemicals, such as MWCNTs. This integrated approach will also be useful for the development of an AOP, when

combining with adverse outcomes at biological levels of organization which are relevant to risk assessment using functional genetics tool, as applied in this study.

Conflict of interest

The authors declare that they have no conflict of interest.

Transparency Document

The Transparency document associated with this article can be found in the online version.

Acknowledgements

This work was supported by Mid-career Researcher Program through the National Research Foundation of Korea (NRF) funded by the Ministry of Science, ICT and Future Planning (2013R1A2A2A03010980) and also by a grant from the Korean Ministry of Environment through National Institute of Environmental Science (NIER) and through "Environmental Health R&D Program" (2012001370009). C.P. Roca and F. Giralt acknowledge support from the EU FP7 project MODERN, Contract No. 309314-2. The authors thank to Prof Robert Rallo at Universitat Rovira i Virgili for his kind reading of the manuscript. *Wildtype (N2)* and mutant strains (described in Table S2) were provided by the CGC, which is funded by NIH Office of Research Infrastructure Programs (P40 OD010440).

Appendix A. Supplementary data

Supplementary data associated with this article can be found, in the online version, at http://dx.doi.org/10.1016/j.cbi.2015.06.031.

References

[1] M.H. Gass, K.K.K. Koziol, A.H. Windle, P.A. Midgley, Four-dimensional spectral tomography of carbonaceous nanocomposites, Nano Lett. 6 (2006) 376–379.
[2] J.M. Schnorr, T.M. Swager, Emerging applications of carbon nanotubes, Chem. Mater. 23 (2011) 646–657.
[3] J. Du, S. Wang, H. You, X. Zhao, Understanding the toxicity of carbon nanotubes in the environment is crucial to the control of nanomaterials in producing and processing and the assessment of health risk for human: a review, Environ. Toxicol. Pharmacol. 36 (2) (2013) 451–462.
[4] C. Ma, W. Zhang, Y. Zhu, L. Ji, R. Zhang, N. Koratkar, J. Liang, Alignment and dispersion of functionalized carbon nanotubes in polymer composites induced by an electric field, Carbon 46 (2008) 706–720.
[5] X. Zhao, R. Liu, Recent progress and perspectives on the toxicity of carbon nanotubes at organism, organ, cell, and biomacromolecule levels, Environ. Int. 40 (2012) 244–255.
[6] K. Donaldson, F.A. Murphy, R. Duffin, C.A. Poland, Asbestos, carbon nanotubes and the pleural mesothelium: a review of the hypothesis regarding the role of long fibre retention in the parietal pleura, inflammation and mesothelioma, Part Fibre Toxicol. 7 (2010) 5.
[7] K. Donaldson, C.A. Poland, F.A. Murphy, M. MacFarlane, T. Chernova, A. Schinwald, Pulmonary toxicity of carbon nanotubes and asbestos - similarities and differences, Adv. Drug Deliv. Rev. 65 (15) (2013) 2078–2086.
[8] C.A. Poland, R. Duffin, I. Kinloch, A. Maynard, W.A. Wallace, A. Seaton, V. Stone, S. Brown, W. Macnee, K. Donaldson, Carbon nanotubes introduced into the abdominal cavity of mice show asbestos-like pathogenicity in a pilot study, Nat. Nanotechnol. 3 (7) (2008) 423–428.
[9] A.R. Reddy, D.R. Krishna, Y.N. Reddy, V. Himabindu, 6504, Toxicol. Mech. Methods 20 (2010) 267–272.
[10] T. Galloway, C. Lewis, I. Dolciotti, B.D. Johnston, J. Moger, F. Regoli, Sublethal toxicity of nano-titanium dioxide and carbon nanotubes in a sediment dwelling marine polychaete, Environ. Pollut. 158 (5) (2010) 1748–1755.
[11] F. Mouchet, P. Landois, P. Puech, E. Pinelli, E. Flahaut, L. Gauthier, Carbon nanotube ecotoxicity in amphibians: assessment of multiwalled carbon nanotubes and comparison with double-walled carbon nanotubes, Nanomedicine 5 (6) (2010) 963–974.
[12] J. Cheng, E. Flahaut, S.H. Cheng, Effect of carbon nanotubes on developing zebrafish embryos, Environ. Toxicol. Chem. 26 (4) (2007) 708–716.
[13] Y. Zhao, Q. Wu, Y. Li, A. Nouara, R. Jia, D. Wang, In vivo translocation and toxicity of multi-walled carbon nanotubes are regulated by microRNAs, Nanoscale 6 (8) (2014) 4275–4284.
[14] R. Klaper, D. Arndt, K. Setyowati, J. Chen, F. Goetz, Functionalization impacts the effects of carbon nanotubes on the immune system of rainbow trout, *Oncorhynchus mykiss*, Aquat Toxicol. 100 (2) (2010) 211–217.
[15] M.C. Leung, J.V. Goldstone, W.A. Boyd, J.H. Freedman, J.N. Meyer, *Caenorhabditis elegans* generates biologically relevant levels of genotoxic metabolites from aflatoxin B1 but not benzo[a]pyrene *in vivo*, Toxicol. Sci. 118 (2) (2010) 444–453.
[16] J. Choi, O.V. Tsyusko, J.M. Unrine, N. Chatterjee, J.M. Ahn, X. Yang, L.B. Thornton, I.T. Ryde, D. Starnes, J.N. Meyer, A micro-sized model for the in vivo studies of nanoparticle toxicity: what has *Caenorhabditis elegans* taught us?, Environ Chem. 11 (3) (2014) 227–246.
[17] G.T. Ankley, R.S. Bennett, R.J. Erickson, D.J. Hoff, M.W. Hornung, R.D. Johnson, D.R. Mount, J.W. Nichols, C.L. Russom, P.K. Schmieder, J.A. Serrrano, J.E. Tietge, D.L. Villeneuve, Adverse outcome pathways: a conceptual framework to support ecotoxicology research and risk assessment, Environ. Toxicol. Chem. 29 (3) (2010) 730–741.
[18] H.C. Wu, X.L. Chang, L. Liu, F. Zhao, Y.L. Zhao, Chemistry of carbon nanotubes in biomedical applications, J. Mater. Chem. 20 (2010) 1036–1052.
[19] D. Tasis, N. Tagmatarchis, A. Bianco, M. Prato, Chemistry of carbon nanotubes, Chem. Rev. 106 (2006) 1105–1136.
[20] S. Vardharajula, S.Z. Ali, P.M. Tiwari, E. Eroğlu, K. Vig, V.A. Dennis, S.R. Singh, Functionalized carbon nanotubes: biomedical applications, Int. J. Nanomed. 7 (2012) 361–5374.
[21] K.K. Jain, Advances in use of functionalized carbon nanotubes for drug design and discovery, Expert Opin. Drug Discov. 7 (11) (2012) 1029–1037.
[22] J.Y. Roh, S.J. Sim, J. Yi, K. Park, K.H. Chung, D.Y. Ryu, J. Choi, Ecotoxicity of silver nanoparticles on the soil nematode *Caenorhabditis elegans* using functional ecotoxicogenomics, Environ. Sci. Technol. 43 (10) (2009) 3933–3940.
[23] L. Shi, L.H. Reid, W.D. Jones, R. Shippy, J.A. Warrington, S.C. Baker, P.J. Collins, F. de Longueville, et al., The microarray quality control (MAQC) project shows inter- and intraplatform reproducibility of gene expression measurements, Nat. Biotechnol. 24 (9) (2006) 1151–1161.
[24] P.H. Chen, K.M. Hsiao, C.C. Chou, Molecular characterization of toxicity mechanism of single-walled carbon nanotubes, Biomaterials 34 (2013) 5661–5669.
[25] S. Pillai, R. Behra, H. Nestler, M.J. Suter, L. Sigg, K. Schirmer, Linking toxicity and adaptive responses across the transcriptome, proteome, and phenotype of *Chlamydomonas reinhardtii* exposed to silver, Proc. Natl. Acad. Sci. U.S.A. 111 (9) (2014) 3490–3495.
[26] J.E. Irazoqui, J.M. Urbach, F.M. Ausubel, Evolution of host innate defence. Insights from *Caenorhabditis elegans* and primitive invertebrates, Nat. Rev. Immunol. 10 (2010) 47–58.
[27] X.W. Wang, N.S. Tan, B. Ho, J.L. Ding, Evidence for the ancient origin of the NF-kappaB/IkappaB cascade: its archaic role in pathogen infection and immunity, Proc. Natl. Acad. Sci. U.S.A. 103 (2006) 4204–4209.
[28] N. Azad, A.K. Iyer, L. Wang, Y. Liu, Y. Lu, Y. Rojanasakul, Reactive oxygen species-mediated p38 MAPK regulates carbon nanotube-induced fibrogenic and angiogenic responses, Nanotoxicology 7 (2013) 157–168.
[29] W.Y. Hsieh, C.C. Chou, C.C. Ho, S.L. Yu, H.Y. Chen, H.Y. Chou, J.J. Chen, H.W. Chen, P.C. Yang, Single-walled carbon nanotubes induce airway hyper reactivity and parenchymal injury in mice, Am. J. Respir. Cell Mol. Biol. 46 (2012) 257–267.
[30] Z. Sun, Z. Liu, J. Meng, J. Meng, J. Duan, S. Xie, X. Lu, Z. Zhu, C. Wang, S. Chen, H. Xu, X.D. Yang, Carbon nanotubes enhance cytotoxicity mediated by human lymphocytes in vitro, PLoS ONE 6 (2011) e21073.
[31] T. Kaletta, M.O. Hengartner, Finding function in novel targets: *C. elegans* as a model organism, Nat. Rev. Drug Discovery 5 (2006) 387–398.
[32] B. Lant, K.B. Storey, An overview of stress response and hypometabolic strategies in *Caenorhabditis elegans*: conserved and contrasting signals with the mammalian system, Int. J. Biol. Sci. 6 (2010) 9–50.
[33] U. Taylor, A. Barchanski, S. Petersen, W.A. Kues, U. Baulain, L. Gamrad, L. Sajti, S. Barcikowski, D. Rath, Gold nanoparticles interfere with sperm functionality by membrane adsorption without penetration, Nanotoxicology 8 (2014) 118–127.
[34] U. Taylor, A. Barchanski, W. Garrels, S. Klein, W. Kues, S. Barcikowski, D. Rath, Toxicity of gold nanoparticles on somatic and reproductive cells, Adv. Exp. Med. Biol. 733 (2012) 125–133.
[35] D. Tiedemann, U. Taylor, C. Rehbock, J. Jakobi, S. Klein, W.A. Kues, S. Barcikowski, D. Rath, Reprotoxicity of gold, silver, and gold-silver alloy nanoparticles on mammalian gametes, Analyst 139 (2014) 931–942.
[36] T. Kirkegaard, A.G. Roth, N.H. Petersen, A.K. Mahalka, O.D. Olsen, I. Moilanen, A. Zylicz, J. Knudsen, K. Sandhoff, C. Arenz, P.K. Kinnunen, J. Nylandsted, M. Jäättelä, Hsp70 stabilizes lysosomes and reverts Niemann-Pick disease-associated lysosomal pathology, Nature 463 (2010) 549–553.
[37] S.S. Mambula, S.K. Calderwood, Heat shock protein 70 is secreted from tumor cells by a nonclassical pathway involving lysosomal endosomes, J. Immunol. 177 (2006) 7849–7857.
[38] B.S. Polla, F. Gabert, B.M. Peyrusse, M.R. Jacquier-Sarlin, Increased proteolysis of diphtheria toxin by human monocytes after heat shock: a subsidiary role for heat-shock protein 70 in antigen processing, Immunology 120 (2007) 230–241.
[39] P.S. Hegde, I.R. White, C. Debouck, Interplay of transcriptomics and proteomics, Curr. Opin. Biotechnol. 14 (2003) 647–651.

[40] C. Núñez, A. Esteve-Núñez, C. Giometti, S. Tollaksen, T. Khare, W. Lin, D. Lovley, R.B.A. Methé, DNA microarray and proteomic analyses of the RpoS regulon in *Geobacter sulfurreducens*, J. Bacteriol. 188 (2006) 2792–2800.
[41] H. Ali-Boucetta, A. Nunes, R. Sainz, M.A. Herrero, B. Tian, M. Prato, A. Bianco, K. Kostarelos, Asbestos-like pathogenicity of long carbon nanotubes alleviated by chemical functionalization, Angew. Chem. Int. Ed. Engl. 52 (8) (2013) 2274–2278.
[42] K.M. Pondman, M. Sobik, A. Nayak, A.G. Tsolaki, A. Jäkel, E. Flahaut, S. Hampel, B. Ten Haken, R.B. Sim, U. Kishore, Complement activation by carbon nanotubes and its influence on the phagocytosis and cytokine response by macrophages, Nanomedicine 10 (6) (2014) 1287–1299.
[43] R. Li, X. Wang, Z. Ji, B. Sun, H. Zhang, C.H. Chang, S. Lin, H. Meng, Y.P. Liao, M. Wang, Z. Li, A.A. Hwang, T.B. Song, R. Xu, Y. Yang, J.I. Zink, A.E. Nel, T. Xia, Surface charge and cellular processing of covalently functionalized multiwall carbon nanotubes determine pulmonary toxicity, ACS Nano 7 (2013) 2352–2368.
[44] X. Li, L. Wang, Y. Fan, Q. Feng, F. Cui, Biocompatibility and toxicity of nanoparticles and nanotubes, J. Nanomater. 548389 (2012) 19.
[45] X. Zhang, Y. Zhu, J. Li, Z. Zhu, J. Li, W. Li, Q. Huang, Tuning the cellular uptake and cytotoxicity of carbon nanotubes by surface hydroxylation, J. Nanopart. Res. 13 (12) (2011) 6941–6952.
[46] Y. Zhao, Q. Wu, Y. Li, D. Wang, Translocation, transfer, and in vivo safety evaluation of engineered nanomaterials in the non-mammalian alternative toxicity assay model of nematode *Caenorhabditis elegans*, RSC Adv. 3 (2013) 5741.
[47] A. Albini, V. Mussi, A. Parodi, A. Ventura, E. Principi, S. Tegami, M. Rocchia, E. Francheschi, I. Sogno, R. Cammarota, G. Finzi, F. Sessa, D.M. Noonan, U. Valbusa, Interactions of single-wall carbon nanotubes with endothelial cells, Nanomedicine 6 (2010) 277–288.
[48] P. Cherukuri, S.M. Bachilo, S.H. Litovsky, R.B. Weisman, Near-infrared fluorescence microscopy of single-walled carbon nanotubes in phagocytic cells, J. Am. Chem. Soc. 126 (2004) 15638–15639.
[49] H. Jin, D.A. Heller, M.S. Strano, Single-particle tracking of endocytosis and exocytosis of single-walled carbon nanotubes in NIH-3T3 cells, Nano Lett. 8 (2008) 1577–1585.
[50] N.W.S. Kam, H. Dai, Carbon nanotubes as intracellular protein transporters: generality and biological functionality, J. Am. Chem. Soc. 127 (2005) 6021–6026.
[51] N.W.S. Kam, T.C. Jessop, P.A. Wender, H. Dai, Nanotube molecular transporters: internalization of carbon nanotube–protein conjugates into mammalian cells, J. Am. Chem. Soc. 126 (2004) 6850–6851.
[52] D. Cai, J.M. Mataraza, Z.H. Qin, Z. Huang, J. Huang, T.C. Chiles, D. Carnahan, K. Kempa, Z. Ren, Highly efficient molecular delivery into mammalian cells using carbon nanotube spearing, Nat. Methods 2 (2005) 449–454.
[53] K. Kostarelos, L. Lacerda, G. Pastorin, W. Wu, S. Wieckowski, J. Luangsivilay, S. Godefroy, D. Pantarotto, J.P. Briand, S. Muller, M. Prato, A. Bianco, Cellular uptake of functionalized carbon nanotubes is independent of functional group and cell type, Nat. Nanotechnol. 2 (2007) 108–113.
[54] X. Wang, Y.C. Wu, V.A. Fadok, M.C. Lee, K. Gengyo-Ando, L.C. Cheng, D. Ledwich, P.K. Hsu, J.Y. Chen, B.K. Chou, P. Henson, S. Mitani, D. Xue, Cell corpse engulfment mediated by *C. elegans* phosphatidylserine receptor through CED-5 and CED-12, Science 302 (2003) 1563–1566.
[55] P.W. Reddien, H.R. Horvitz, CED-2/CrkII and CED-10/Rac control phagocytosis and cell migration in *Caenorhabditis elegans*, Nat. Cell Biol. 2 (2000) 131–136.
[56] Y.C. Wu, H.R. Horvitz, *C. elegans* phagocytosis and cell-migration protein CED-5 is similar to human DOCK180, Nature 392 (1998) 501–504.
[57] Y.C. Wu, M.C. Tsai, L.C. Cheng, C.J. Chou, N.Y. Weng, *C. elegans* CED-12 acts in the conserved crkII/DOCK180/Rac pathway to control cell migration and cell corpse engulfment, Dev. Cell 1 (2001) 491–502.
[58] J.O. Agola, L. Hong, Z. Surviladze, O. Ursu, A. Waller, J.J. Strouse, D.S. Simpson, C.E. Schroeder, T.I. Oprea, J.E. Golden, J. Aubé, T. Buranda, L.A. Sklar, A. Wandinger-Ness, A competitive nucleotide binding inhibitor: in vitro characterization of Rab7 GTPase inhibition, ACS Chem. Biol. 7 (6) (2012) 1095–1108.
[59] S.L. Schwartz, C. Cao, O. Pylypenko, A. Rak, A. Wandinger-Ness, Rab GTPases at a glance, J. Cell Sci. 120 (Pt 22) (2007) 3905–3910.
[60] X. Yu, S. Odera, C.H. Chuang, N. Lu, Z. Zhou, *C. elegans* dynamin mediates the signaling of phagocytic receptor CED-1 for the engulfment and degradation of apoptotic cells, Dev. Cell 10 (6) (2006) 743–757.
[61] X. Yu, N. Lu, Z. Zhou, Phagocytic receptor CED-1 initiates a signaling pathway for degrading engulfed apoptotic cells, PLoS Biol. 6 (3) (2008) e61.
[62] K. Peynshaert, B.B. Manshian, F. Joris, K. Braeckmans, S.C. De Smedt, J. Demeester, S.J. Soenen, Exploiting intrinsic nanoparticle toxicity: the pros and cons of nanoparticle-induced autophagy in biomedical research, Chem. Rev. 114 (15) (2014) 7581–7609.
[63] B. Grant, Y. Zhang, M.C. Paupard, S.X. Lin, D.H. Hall, D. Hirsh, Evidence that RME-1, a conserved *C. elegans* EH-domain protein, functions in endocytic recycling, Nat. Cell Biol. 3 (2001) 573–579.
[64] B. Grant, D. Hirsh, Receptor-mediated endocytosis in the *Caenorhabditis elegans* oocyte, Mol. Biol. Cell 10 (1999) 4311–4326.
[65] Y. Zhang, B. Grant, D. Hirsh, RME-8, a conserved J-domain protein, is required for endocytosis in *Caenorhabditis elegans*, Mol. Biol. Cell 12 (2001) 2011–2021.
[66] B.K. Choi, D.J. Chitwood, Y.K. Paik, Proteomic changes during disturbance of cholesterol metabolism by azacoprostane treatment in *Caenorhabditis elegans*, Mol. Cell. Proteomics 2 (2003) 1086–1095.
[67] R. Zhang, M.J. Piao, K.C. Kim, A.D. Kim, J.Y. Choi, J. Choi, J.W. Hyun, Endoplasmic reticulum stress signaling is involved in silver nanoparticles-induced apoptosis, Int. J. Biochem. Cell Biol. 44 (1) (2012) 224–232.
[68] O.V. Tsyusko, J.M. Unrine, D. Spurgeon, E. Blalock, D. Starnes, M. Tseng, G. Joice, P.M. Bertsch, Toxicogenomic responses of the model organism *Caenorhabditis elegans* to gold nanoparticles, Environ. Sci. Technol. 46 (2012) 4115–4124.
[69] Z. Kostova, D.H. Wolf, For whom the bell tolls: protein quality control of the endoplasmic reticulum and the ubiquitin-proteasome connection, EMBO J. 22 (2003) 2309–2317.
[70] C. Koumenis, ER stress, hypoxia tolerance and tumor progression, Curr. Mol. Med. 6 (2006) 55–69.
[71] J. Guo, H.Y. Nie, H.F. Wang, G. Jia, The cytotoxicity and expression changes of endoplasmic reticulum related genes induced by MWCNTs with different surface modifications, Beijing Da Xue Xue Bao 43 (2011) 342–347.
[72] X. Wang, J. Guo, T. Chen, H. Nie, H. Wang, J. Zang, X. Cui, G. Jia, Multi-walled carbon nanotubes induce apoptosis via mitochondrial pathway and scavenger receptor, Toxicol. In Vitro 26 (2012) 799–806.
[73] X. He, S.H. Young, D. Schwegler-Berry, W.P. Chisholm, J.E. Fernback, Q. Ma, Multiwalled carbon nanotubes induce a fibrogenic response by stimulating reactive oxygen species production, activating NF-κB signaling, and promoting fibroblast-to-myofibroblast transformation, Chem. Res. Toxicol. 24 (2011) 2237–2248.
[74] R.K. Srivastava, A.B. Pant, M.P. Kashyap, V. Kumar, M. Lohani, L. Jonas, Q. Rahman, Multi-walled carbon nanotubes induce oxidative stress and apoptosis in human lung cancer cell line-A549, Nanotoxicology 5 (2011) 195–207.
[75] S.F. Ye, Y.H. Wu, Z.Q. Hou, Q.Q. Zhang, ROS and NF-kappaB are involved in upregulation of IL-8 in A549 cells exposed to multi-walled carbon nanotubes, Biochem. Biophys. Res. Commun. 379 (2009) 643–648.